ELECTROANALYSIS
An International Journal Devoted to Electroanalysis, Sensors and Bioelectronic Devices

Accepted Article

Title: Electrochemical Aptasensors for Biological and Chemical Analyte Detection

Authors: Seda Nur Topkaya and Arif Cetin

To be cited as: *Electroanalysis* 10.1002/elan.202060388

Link to VoR: https://doi.org/10.1002/elan.202060388

WILEY-VCH

10.1002/elan.202060388

Electrochemical Aptasensors for Biological and Chemical Analyte Detection

Seda Nur Topkaya [1*], Arif E. Cetin [2]

[1] Izmir Katip Celebi University, Faculty of Pharmacy, Department of Analytical Chemistry, Izmir, Turkey

[2] Izmir Biomedicine and Genome Center, Izmir, Turkey

***Address:** Izmir Katip Celebi University, Faculty of Pharmacy, Department of Analytical Chemistry, 35620, Cigli, Izmir, TURKEY.

E-mail: sedanur6@gmail.com, sedanur.topkaya@ikcu.edu.tr

ABSTRACT

Aptamers are short length, single-stranded DNA or RNA affinity molecules which interact with any desired targets such as biomarkers, cells, biological molecules, drugs or chemicals with high sensitivity. They have been extensively employed for medical applications due to having more advantages than the antibodies such as easier preparation and modification, higher stability, lower batch-to-batch variability and cost. Moreover, aptamers can be easily integrated efficiently with sensors, biosensors, actuators and other devices.

In this review article, different applications of aptamers for biological and chemical molecules detection within the scope of electrochemical methods were presented with recent studies. In addition, the present status and future perspectives for highly-effective aptasensors for specific and selective analyte detection were discussed. As in stated throughout the review, combining of extraordinary properties of aptamers with the electrochemical-based biosensors could have improved the sensitivity of the assay and reduced limit of detection.

Keywords: Electrochemical Biosensors, Aptasensors, Biomarker Detection, Small Molecules, Voltammetry, Affinity Sensors.

1. INTRODUCTION

Aptamers are defined as single-stranded deoxyribonucleic acid (ssDNA) or ribonucleic acid (RNA) that can bind specifically to target with high affinity and selectivity [1]. Their high affinity arise from their capability of folding upon their target molecules such as proteins, biomarkers, carbohydrates, cells, tissues, small molecules, heavy metals or toxins. Aptamers are short length oligonucleotides and they can easily form into secondary structures such as hairpin, stem, loop, bugle and G-quadruplex and these formations play a critical role in recognition-based binding activity between aptamer and its target [2]. Aptamers are generally considered as ***artificial antibodies*** which act similar to antibodies but provide better advantages. The reason of comparing of aptamers with the antibodies is that the both molecules function as affinity agents. Unlike antibodies, aptamers are synthetically manufactured without batch-to-batch differences [3]. Additionally, antibodies are able to bind to larger molecules, while aptamers can interact to smaller molecules [4]. Moreover, aptamers are more flexible than antibodies and oligonucleotide-based aptamers are more thermally stable than the protein based antibodies at elevated temperatures. The most significant advantage of aptamers to antibodies is that antibodies with large size cannot penetrate into tumors or tissues deeply and result in lower therapeutic and imaging efficiency. A comparison of aptamers with antibodies was presented in Table 1.

Table 1: Comparison of aptamers and antibodies in terms of target type, synthesis time, stability, size, chemical modification, production, cost and toxicity.

FEATURES	APTAMERS	ANTIBODY
Target Type	Even the toxic molecules	Non-toxic molecules
Synthesis Time	Days or weeks	Months
Stability	At ambient temperature	Low temperature
Size	Smaller	Relatively larger
Chemical Modification	Easy	Difficult, limited
Production	In vitro	In vivo
Cost	Cost-effective	Expensive
Toxicity	Not observed	Immune reaction observed

Although aptamers have remarkable advantages, they have also some limitations. Aptamers are highly responsive to environmental changes, i.e., ionic strength, pH and temperature due to their physical properties such as their short lengths. Therefore, experimental conditions can drastically affect target binding efficiency. Thus, the experimental factors should be carefully optimized to develop robust and stable aptamers for specific analytical applications. The main limitation of aptamers is their sensitivity to nuclease activity. Moreover, response of aptamers and their sensitivity may differ on different surfaces [5].

Aptamers are isolated with ***'Systematic Evolution of Ligands by Exponential Enrichment' (SELEX)*** selection process by applying a repeated process of in vitro selection and amplification [6]. SELEX contains three main steps: ***binding, partitioning and amplification*** (Figure 1A). Target molecules are incubated with a random library in the binding step. In the second part of SELEX, target bound aptamers are separated from unbound ones and finally selected aptamers are amplified by Polymerase Chain Reaction (PCR) to be used in the next round of selection. These steps are repeated several times (generally 6-10) and then target ligand is collected. The steps for SELEX process was shown in Figure 1A. Success of SELEX process rely on many factors such as aptamers library, physical and chemical characteristics of the target molecules, purity of the target and aptamers enrichment assays. In addition, the use of proper enzymes and their combinations for amplification and pool production affect the SELEX success [5]. After SELEX, candidate aptamers are identified with high-throughput sequencing methods which are really labor intensive and time consuming. Recently, bioinformatics analysis are also conducted for identifying process. Once the candidate aptamers are analyzed, they are further tested to evaluate their binding affinity, specificity and stability. In recent years, efforts have been turning to maximize structural contacts between the aptamers and analytes to improve sensitivity and selectivity. For instance, computational studies of primary and secondary structures to describe oligonucleotides for better aptamers qualities are preferred before or after SELEX [7]. In years, SELEX have been modified with many techniques such as capture-SELEX [8], cell-SELEX [9], immunoprecipitation-coupled SELEX (IP-SELEX) [10], capillary electrophoresis-SELEX (CE-SELEX) [11] and microfluidic SELEX [12]. Cell-SELEX process was shown in Figure 1B.

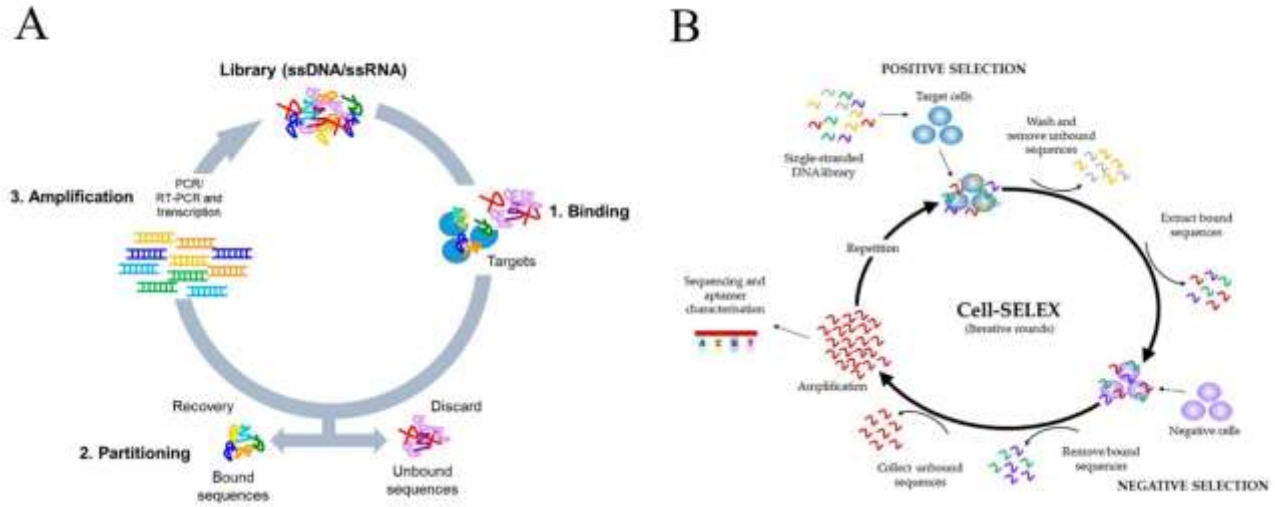

Figure 1: (A) The steps for general SELEX process: binding, partitioning and amplification (Reprinted from [13] with permission: ©2017 MDPI AG). **(B)** Cell-SELEX process (Reprinted from [14] with permission: ©2017 MDPI AG).

Aptamers, which are authentic analytical tools, have been used for a wide range of functions from basic research to commercial applications. They have been widely used to design sensors and biosensors due to their easy adaptability to different platforms [15]. Especially, using an aptamer within a biosensor system has received significant attention for quantitative or semi-quantitative analysis of biological targets. ***Aptasensors*** are the biosensor systems with aptamer components [16]. The underlying mechanism of biosensing is the presence of an analyte, pairing with aptamers that causes structural rearrangements and conformational changes of aptamers that leads to a signal change. The most attractive feature of aptamers is that they can be easily modified with various labels such as fluorescence tags, quenchers, indicators, nanomaterials or enzymes. Aptasensors can be classified based on their transducer types such as electrochemical, optical, colorimetric, mass sensitive or thermal. Analytes binding to aptamers cause conformational changes in aptamers structures, that trigger signals detected by means of transducers. Especially, electrochemical transducers have received significant attention for biomarker detection, targeted therapeutics and molecular diagnostics thanks to their ability of multiple detection, providing rapid and low-cost analysis, the need for minimal labor and low sample volumes [17]. The data for concentration, reaction kinetics and mechanisms, chemical status and other behavior of species in solution can be easily analyzed with electrochemical methods. Therefore, these kinds of transducers have been used in large numbers of clinical assays. Electrochemical transducers could measure current, potential, conductance or resistance and provide information of electrical signals that are proportional to analyte concentration. However, converting biological information aroused from an interaction to electronical signals is highly troublesome due to the complex structure of an electronic device [18].

Amperometry measures the potential differences between indicator and reference electrodes at a constant potential. Chemical molecules are either oxidized or reduced at inert electrodes at constant potential. Amperometry generally provides lower detection limits, but its usage is restricted to electroactive species. Amperometric systems are generally used in enzyme-based sensors, where the enzyme catalyzes a redox reaction [19].

Voltammetry measures the resulting current of an electrochemical cell as a function of a time-dependent potential. In voltammetry, applied potential can be changed and the obtained current can be recorded over a period of time. In voltammetric measurements, three electrode system generally are used. Voltammetric methods are subdivided into Cyclic Voltammetry (CV), Differential Pulse Voltammetry (DPV), Alternating Current Voltammetry (ACV), Linear Sweep Voltammetry (LSV), Anodic Stripping Voltammetry (ASW), Cathodic Stripping Voltammetry (CSW) and Square Wave Voltammetry (SWV). Voltammetric measurements mainly provide quantitative and qualitative results about the oxidation or reduction reactions both directly and indirectly [20].

Potentiometry measures the potential of two-electrode system in the absence of current flow. As a result of this absence, its composition remains unchanged. One of the most preferred potentiometric based sensors, ion-selective electrodes (ISEs), have been used widely as a straightforward and powerful tools for evaluating the activity of ions in variety of samples including biological, chemical and environmental ones. ISEs enable selective detection of ions in the presence of other substances and offers a cost-effective platform. One of the well-known applications of potentiometry is measuring pH of solutions. In addition, trace metal analysis with potentiometric methods have been widely used for environmental applications.

Electrochemical impedance spectroscopy (EIS) analyzes the alternative current (AC) response as a function of frequency. EIS data are analyzed using the changes in the current/potential at the measured frequencies, which determines the electrochemical behavior of the electrodes. EIS which is a responsive and non-damaging technique, has been widely employed in different reactions and interfaces such as corrosion, coatings, conductors, batteries, fuel cells and electrocatalytic reactions as well as characterization of interface properties of biosensors [21]. The most significant feature of EIS method is to eliminate the need for the labeled electroactive groups or indicators. However, EIS is a complementary technique, and other analyze methods should also be used to interpret the interfacial processes.

In this review, the use of aptamers to detect biologically important analytes, biomarkers and small molecules i.e., drugs or organic molecules with electrochemical methods were presented. In addition, the present challenges and future perspectives for developing novel highly-effective aptasensors for analyte detection were discussed.

2. APTASENSORS FOR BIOLOGICAL ANALYTES DETECTION

In recent years, several electrochemical aptasensors have been developed to detect specific cells, biological molecules, biomarkers, proteins, genes, enzymes and hormones with EIS [22], SWV [23], DPV [24], CV [25] and chronocoulometry [26]. Especially, biomarkers have been a significant focus of aptasensors. Biomarkers; including cells, proteins, and nucleic acids, are the molecules with abnormal expression, activity or inactivity which would be observed in pathologic conditions. Therefore, they can be used as indicators for evaluation of either normal or pathologic conditions. The use of aptamers for biomarker detection especially in cancer disease has been rising due to their selective target affinity and enabling of chemical modification. Aptamers could also detect slight differences between proteins with similar structure, and this unique feature enables aptamers to distinguish cancer cells from the healthy ones. However, selectivity is still a concern for cancer aptasensors due to the complex environment of cancer cells. Moreover, the concentrations of disease-related biomarkers generally cannot be detected at first phases of the disease. Thus, the detection of the disease related biomarkers as early as possible with lower concentrations are highly desirable.

Recently, magnetic beads and nanoparticles based test are great of interest due to easy integration of these methods with microfluidics systems. In a recent study, conversion of exosome detection to nucleic acid detection was achieved [27]. First, three kinds of messenger DNAs (mDNAs) were released by means of aptamer-magnetic bead bioconjugates capturing tumor exosomes. In the presence of target exosomes, aptamers were recognized and bound to the target and mDNAs were released. Then, separation was achieved magnetically and released mDNAs hybridized with probe DNA. The assembled structure was mounted on surface of the gold electrodes. Then, cyclic enzymatic amplification method was employed to detect the released mDNAs. As an hybridization indicator, electroactive $Ru(NH_3)_6^{3+}$ current signal was evaluated due to its electrostatic attraction to DNA. Tumor exosomes were detected with the decrease in the signal of $Ru(NH_3)_6^{3+}$, which was correlated with mDNA concentration and the exosome concentration. The relationship between $Ru(NH_3)_6^{3+}$, mDNA and tumor exosomes enabled a successful target detection as 70 particles/μL.

Aptamers have unique adaptabilities for different platforms and signaling modalities. For instance, researchers developed a novel and label-free transporter system which is composed of aptamer and nanomotor for the conveying of Human Promyelocytic Leukemia Cells (HL-60) [28]. In this study, nanomotors were formed of manganese oxide nanosheets and polyethyleneimine decorated with nickel/gold nanoparticles (MnO_2-PEI/Ni/Au). Then, the nanomotors were transported to thiol-tagged aptamer solution. The magnetic stand in a vial was used to separate the aptamer-modified self-propelled nanomotors. Then, the resulting aptamer/nanomotors were used for transporting HL-60 cancer cells from serum samples. For this purpose, complementary nucleotide sequences were added to the buffer solution, containing HL-60/aptamers/nanomotors to release HL-60 cancer cells. The experimental steps were shown in Figure 2A. Different concentration of HL-60 cancer cells in serum samples were also determined by EIS. The proposed aptamer based method is efficient, economic and easy to apply for the bulk fabrication of nanomotor. The LOD was found as 250 cells/mL.

In other study, sandwich-type amperometric aptasensor was developed for the detection of human leukemic lymphoblasts (CCRF-CEM) by using a flow injection) [29]. First, poly (3,4-ethylenedioxythiophene) decorated with gold nanoparticles (PEDOT-AuNPs) was manufactured for immobilization of thiolated aptamers. Multi-walled carbon nanotubes (MWCNTs) were then incorporated with palladium nanoparticles/3,4,9,10-perylene tetracarboxylic acid (MWCNTs-Pdnano/PTCA) to construct the catalytic labeled aptamer. The fabrication process was shown in Figure 2B. When the aptamer was attached to the target, it catalyzed the electroactive molecules, e.g., hydrogen peroxide (H_2O_2), and enhanced the signals that depend on the target concentration. The LOD was found as 8 cells/mL.

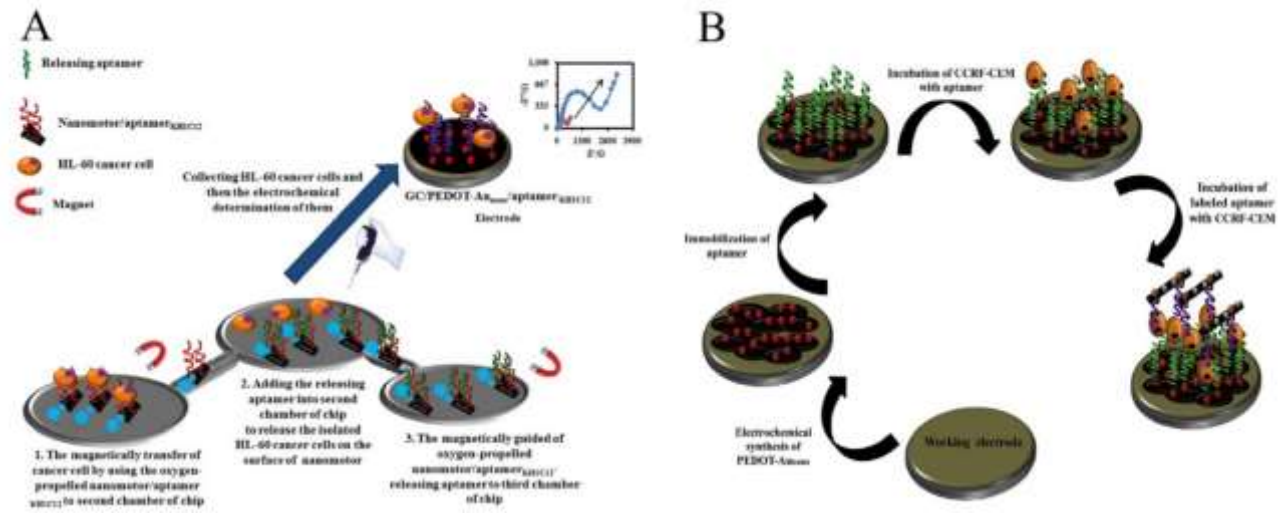

Figure 2: (A) Presentation of isolation and determination of HL-60 cells using aptamer-modified self-propelled nanomotors **(**Reprinted from [28] with permission: ©2018 Elsevier B.V.). **(B)** Presentation of fabrication of sandwich-type aptasensor (Reprinted from [29] with permission: ©2017 Elsevier B.V.).

An electrochemical aptasensor for the detection of released vascular endothelial growth factor (VEGF) and prostate-specific antigen (PSA) from RWPE-1, LNCaP and PC3prostate cell lines was developed by using SWV and EIS [30]. The principle was the self-assembly of thiolated aptamers on the gold-coated silicon (working electrode). Methylene blue (MB) was used as redox indicator. The homogeny immobilization of the aptamer to the surface was confirmed via Surface Plasmon Resonance (SPR) system. In the study, binding of VEGF to the aptamer caused unfolding of DNA hairpin structure, which caused to reduced electron transfer rate from MB to the electrode. The LOD was calculated as 0.08 ng/ mL and 0.15 ng/mL for PSA and VEGF respectively within a linear range of 0.15–100 ng/mL.

As it is known, EIS can be used for protein and other biological based molecules analysis since proteins can lead remarkable changes in the charge transfer resistance (R_{ct}) when immobilized on the electrode. To detect PSA, a polyaniline (PANI) and gold nanoparticles (AuNPs) based amino-functionalized aptasensor was developed utilizing EIS [31]. In the study, PANI and AuNPs modified electrodes were coated with peptides as the antifouling agents reduce nonspecific adsorption. 1-Ethyl-3-(3-dimethylaminopropyl) carbodiimide (EDC) and N-hydroxysuccinimide (NHS) chemistry was applied to activate the carboxyl groups of the peptide. The schematic steps were shown in Figure 3A. The R_{ct} values of working electrodes coated with the PANI/AuNPs/Peptide and PANI/AuNPs/Peptide/PSA aptamer were compared (Figure 3B). When working electrode was modified with PANI and AuNPs, R_{ct} reduced due to the enhanced electron transfer. When PANI/AuNPs modified electrodes coated with peptide, R_{ct} increased due to the non-conductive nature of peptide. Addition of aptamer to the modified electrodes caused R_{ct} values to increase. The variations within the R_{ct} value enabled the quantitative determination of PSA. LOD was found as 0.085 pg/ mL within a linear range of 0.1 pg/mL-100 ng/mL.

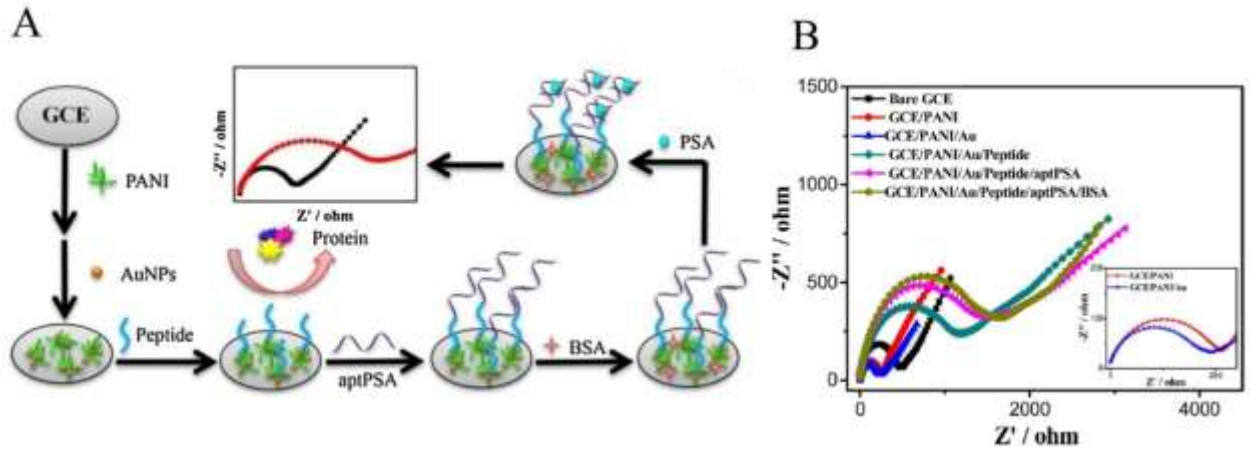

Figure 3: (A) Schematic presentation of detection of PSA biomarker by using an electrochemical system **(B)** EIS spectra of bare and different modified electrodes in 5.0 mM $[Fe(CN)_6]^{3-/4-}$ (Reprinted from [31] with permission: ©2019 Elsevier B.V.).

As an example of electrochemical aptasensors for detecting an important biomarker of inflammation, researchers investigated the interaction of surface-tethered RNA aptamer and C-Reactive Protein (CRP) with voltammetric methods [32]. The use of a thiolated RNA aptamer as a receptor element enabled higher surface coverage in comparison to unmodified surfaces. MB was used to monitor the interaction between the aptamers and the analyte. MB current decreased linearly with increased CRP concentration. LOD was found as 5 pg/L. The interaction between the aptamer and its target was also supported with quartz crystal microbalance (QCM) measurements.

Another study tried to solve the selectivity problem of aptasensors by developing a label-free detection strategy using TLS11a aptamers (APT) that binds to the membrane surface of hepatocellular carcinoma (HepG2) cells [33]. Before sending the APT, the gold electrode (GE) surface was incubated with 3-mercaptopropionic acid (MPA) to prevent non-specific interactions. HepG2 cells were then captured with a sandwich architecture using amino-labeled APT covalently attached to the electrode and a secondary APT. The experimental steps were shown in Figure 4A. The interaction was detected with CV (Figure 4B) and EIS (Figure 4C-D). Using of APT as a recognition layer caused the detection HepG2 cancer cells with high affinity compared to control. The LOD was found as 2 cells/mL with a wide linear dynamic range over 10^2 to 10^6 cells/mL (Figure 4E).

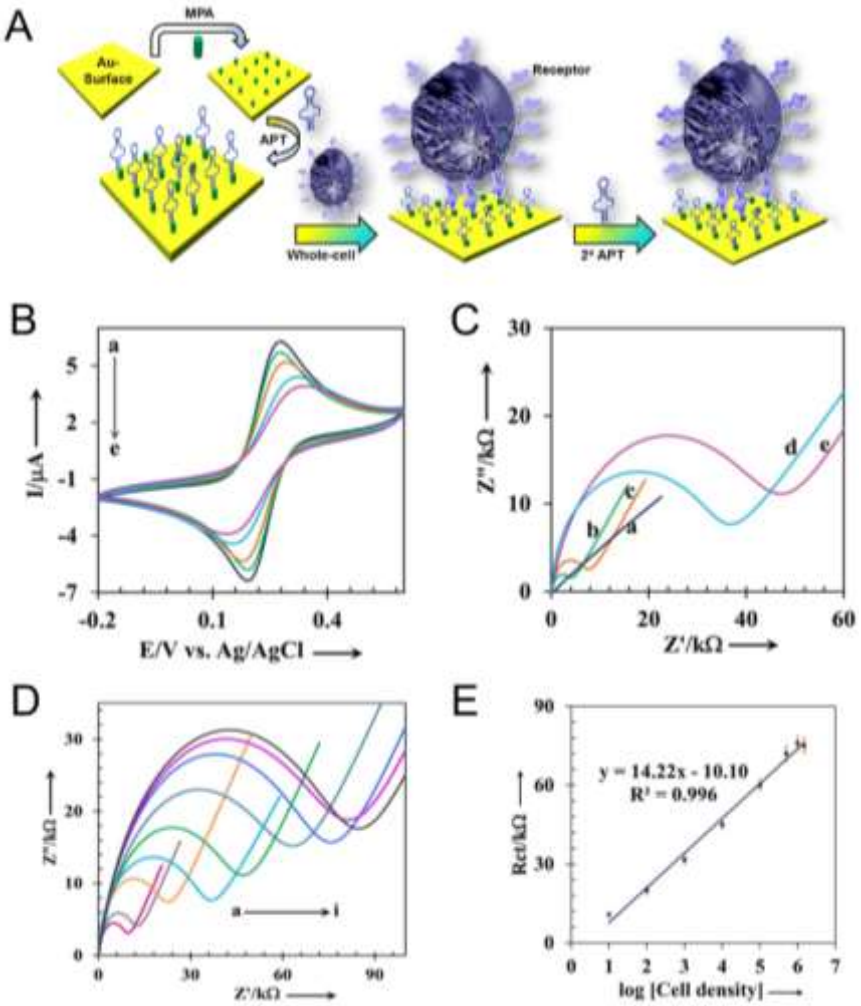

Figure 4: (A) Schematic presentation of TLS11a aptamer and its interaction with HepG2 cells. **(B)** CV and **(C)** Nyquist plots for (a) bare GE, (b) GE/MPA, (c) GE/MPA/APT (d) GE/MPA/APT/HepG2 cell, (e) GE/MPA/APT/HepG2/APT **(D)** Nyquist plots in the same conditions of A and B, (a−i) GE/MPA/APT/cell/APT (0, 10, 10^2, 10^3, 10^4, 10^5, 5×10^5, 10^6 and $1.5x10^6$ HepG2 cells/mL). **(E)** Calibration plots for the developed aptasensor (Reprinted from [33] with permission: ©2014 American Chemical Society).

In another selective biomarker detection study, a magnetoelectrochemical aptasensor was developed for the detection of PSA with silver/cadmium oxide nanoparticles (Ag/CdO NPs) to benefit from the nanomaterials' properties such as small size, high surface to volume ratio and quantum tunneling effect. [34]. In the study, aptamer-modified nanoparticles were immobilized on the surface of superparamagnetic Fe_3O_4/graphene oxide nanosheets through the hydrophobic and pi-pi stacking. The assembly provided better electrochemical properties, efficient electron transfer and super-paramagnetic responses. LOD was found as 28 pg/mL.

Liu et al. developed a modified electrode system consisted of gold nanoparticles (AuNPs), thionine and multi-walled carbon nanotubes (AuNPs-Thi-MW-CNTs) to detect 17-estradiol in real samples with an aptamer based system using DPV, CV and EIS [35]. First, CNTs were loaded with Thi and then AuNPs were decorated on the surface of CNTs by adding Thi-CNTs solution into AuNPs solution. After assembling the electrodes, Tris(2-carboxyethyl)phosphine hydrochloride (TCEP) mixed with DNA aptamer to decrease the possible disulfide bonds in aptamer to thiols and a constant potential of +0.4 V was applied to the electrode. Trace analysis of 17β-estradiol in real samples was achieved with 1.5 pM detection limit.

Another interesting study was conducted for diagnosing periodontal diseases in early phases to detect Human Odontogenic Ameloblast-Associated protein (ODAM). ODAM is a highly specific biomarker for periodontal diseases in gingival crevicular fluid (GCF) from the saliva [36]. In the study, a pair of aptamers binding to ODAM with graphene oxide-based SELEX (GO-SELEX) method was used. Selected aptamers were then characterized with GO-based fluorescence resonance energy transfer (GO-FRET) due to the benefiting from GO's quenching fluorescence signal. SPR was also employed to characterize the method by immobilizing aptamers onto the gold chip surface via avidin-biotin linkage. LOD was found as 1.63 nM in saliva samples.

An ultrasensitive amperometric aptasensor based on SWV was developed for determination of a transmembrane glycoprotein, Epithelial Cell Adhesion Molecule (EpCAM), a cancer biomarker which involves cell signaling process [37]. EpCAM is secreted at low levels from normal cells, however it is overexpressed in cancer cells, so its sensitive and quantitative detection is under interest. In the study, toehold-mediated DNA recycling amplification was achieved by using toehold domain that was a short stretching single-stranded region (nearly 5–8 nucleotides) and a trigger for initiating hybridization. First, hairpin probe 1 (Hp1) with a toehold region was modified with a 5′-thiol (5'-SH) and immobilized onto the gold electrode. Before adding EpCAM, the probe A was hybridized with aptamer to form aptamer/probe A duplex. After addition of analyte, probe A was released from the aptamer/probe duplex and hybridized with the Hp1 toehold domain. The reaction resulted in further hybridizing with hairpin probe 2 (Hp2) to displace probe A in the presence of Hp2. Hp2 was labeled with the redox indicator MB. Subsequently, released probe A was hybridized with another Hp1 to start the next round of DNA recycling amplification by reusing probe A. Formation of many MB-labeled DNA strands on the electrode surface generated enhanced currents measured with SWV. The designed method was successful for the determination of EpCAM. LOD was found as 20 pg/mL. The schematic illustration and the current signals obtained from SWV measurements were shown in Figure 5.

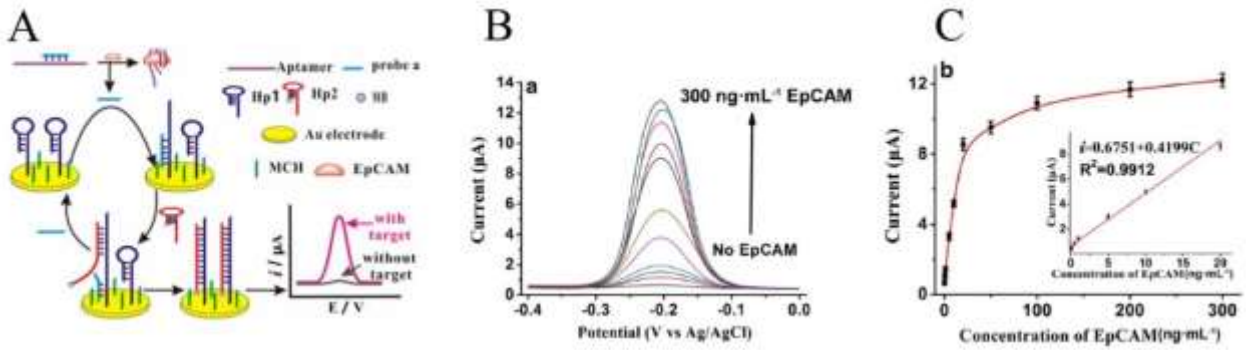

Figure 5: (A) Schematic presentation of an aptasensor to detect EpCAM molecule via DNA recycling amplification **(B)** Current signals obtained from different concentrations of EpCAM in the presence of EpCAM aptamer/probe A and Hp2 (from bottom to top: 0 to 300 ng/mL) by using SWV measurements. **(C)** Calibration curve of different concentrations of EpCAM. (Hp1: Hairpin probe 1; Hp2: Hairpin probe 2; MB: Methylene blue; MCH: 6-Mercapto-1-hexanol; EpCAM: Epithelial cell adhesion molecule). (Reprinted from [37] with permission: ©2020 Springer Nature Switzerland AG.).

One of the most used detection strategy with aptasensor design is the signal-ON/OFF principle. In general, aptamers are functionalized with a redox indicator. When analyte and aptamer interacts, a conformational change occurs and results in a change in the electron transfer between an indicator and an electrode [38]. The signal-ON/OFF based aptasensor systems causes to increase or decrease of the signal of the redox probe after the target interaction which allows real-time analysis and simultaneous multi-analyte detection. However, the conformation of aptamer-redox probe-target is highly sensitive to environmental changes and composition of the sample. Thus, experimental conditions should be properly adjusted when using these kind of aptasensors systems. The principles of the methodology was shown in Figure 6.

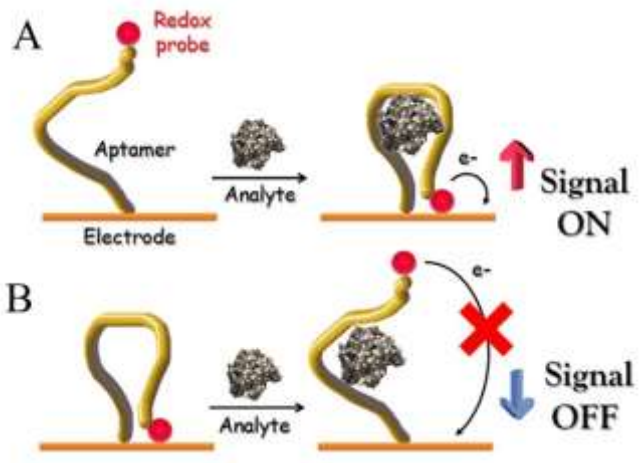

Figure 6: The main principle of the (A) signal-ON and (B) signal-OFF strategy in electrochemical aptasensors (Reprinted from [38] with permission: ©2020 Springer Nature Switzerland AG.).

In an amperometric and signal-ON/OFF based study, gold-silica anisotropic nanomaterials, Janus nanoparticles, were used as a bio-recognition-signaling element for the detection of carcinoembryonic antigen (CEA) biomarker. At first step, Janus nanoparticles were functionalized with horseradish peroxidase (HRP) enzyme and immobilized on the silica surface. Afterwards, a biotin thiol-modified aptamer were sent onto gold surface as bio-recognition element. The unique design enabled unfolding of DNA hairpin structure and unmasking the biotin residues at the aptamer chain (Figure 7). Finally, nanoparticle/aptamer structure was captured by avidin-modified Fe_3O_4@SiO_2. Fe_3O_4 particles were used for achieving magnetic deposition on screen-printed carbon electrodes (OHT-000) surface. They called the modified electrode as avidin-modified magnetic NanoCaptors (NCR-80). In Figure 7-Step A, addition of H_2O_2 and hydroquinone (HQ) caused by the reduction of the oxidized form of the electrochemical mediator formed in the HRP-catalyzed reaction (signal-ON). In Step B, amperometric signals obtained without CEA (signal-OFF). The designed assembly successfully detected CEA biomarker within a linear range of 1-5000 ng/mL with a LOD of 1.2 pM in serum samples [39].

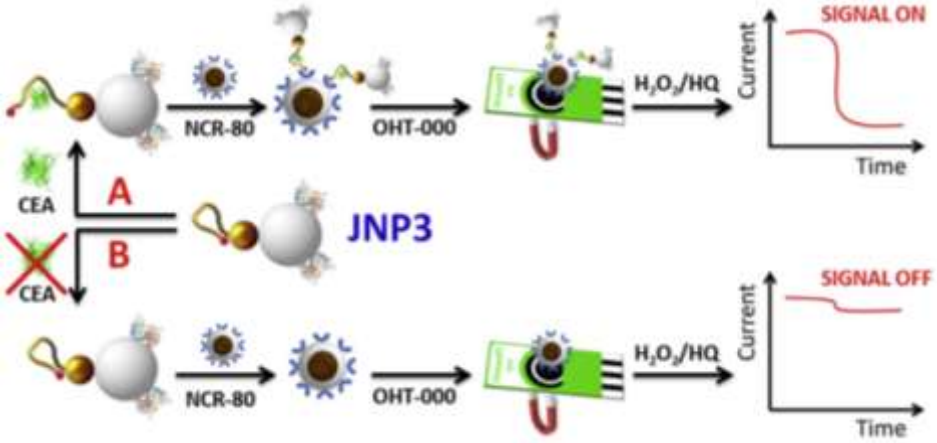

Figure 7: Schematic representation of the Janus nanoparticles-based detection for CEA biomarker by using NCR-80 and OHT-000) (Reprinted from [39] with permission: ©2019 Elsevier B.V.).

In recent years, the demand for non-invasive, accurate and highly specific biomarkers have been rising due to the complex nature of the cancer disease. One of the promising tumor biomarkers, circulating tumor cells (CTCs), have been gaining great interests due to providing useful information on metastatic risk, disease progression and treatment effectiveness. CTCs are tumor components such as whole single cells and cell clusters released from tumors into the blood. In order to detect CTCs, a procedure was developed by using an array nanochannel-ion channel hybrid combined with an electrochemical analysis method. In the study, the specific aptamer probe was immobilized to the surface of ion-channel to capture CTCs [40]. The captured cells effectively covered the entry of ion channels, which completely blocked the ionic flow via the channels leading to an altered mass transfer property. The mass transfer properties were analyzed with LSV and LOD was found as 100 cells/mL.

Examples of aptasensors for detecting different types of biological analytes and their sensitivities are listed in Table 2.

Table 2: Electrochemical based aptasensors for detecting different types of biological analytes and their respective sensitivities.

METHOD	ANALYTE	TARGET	LOD	REFERENCE
DPV	HeLa	Cell	10 cell/mL	[41]
DPV	K562	Cell	14 cell/mL	[42]
DPV	CCRF-CEM	Cell	10 cell/mL	[43]
EIS, CV	MCF-7	Cell	8 cell/mL	[44]
EIS	MCF-7	Cell	36 cell/mL	[45]
DPV and EIS	PSA	Biomarker	1 pg/mL	[46]
DPV	EGFR	Biomarker	50 pg/mL	[47]
EIS	PSA	Biomarker	5 pg/mL	[48]
CV, EIS	Serpin A12	Biomarker	0.031 ng/mL	[49]
EIS, CV, DPV	MUC1	Biomarker	0.62 ppb	[50]
EIS	Cardiac Troponin I	Biomarker	1.23 pM	[51]
DPV	Cardiac troponin I	Biomarker	16 pg/mL	[52]
Amperometry	Interleukin 6	Biomarker	0.33 pg/mL	[53]
Amperometry	Human Factor IX	Biomarker	6 pM	[54]
DPV, EIS	Alpha-fetoprotein	Protein	61.8 fg/mL	[55]
EIS	Thrombin	Protein	10 pM	[56]
DPV	Insulin	Hormone	0.18 fM	[57]
CV, EIS	Thyroxine (T4)	Hormone	10.33 pM	[58]
CV, EIS	Progesterone (P4)	Hormone	1.86 pM	[59]

Abbreviations: LOD: Limit of Detection; **EIS:** Electrochemical Impedance Spectroscopy; **ASV:** Anodic Stripping Voltammetry; **CV:** Cyclic Voltammetry; **DPV:** Differential Pulse Voltammetry; **PSA:** Prostate Specific Antigen; **EGFR:** Epidermal Growth Factor Receptor; **MUC1:** Mucin1.

Regardless of the significant and remarkable progresses in the development of novel aptasensors, most of these platforms are still able to detect only one analyte. Biological fluids including saliva, blood, blood plasma, urine and cerebrospinal fluid are pretty complex samples contain impurities that may cause inaccurate detection of the analytes. Thus, developing novel and highly specific in a complex environment is needed. For this purpose, an aptansensor have been developed to detect cancer biomarkers, CEA and MUC1, in real samples. Two different aptamers labeled with redox tags were used as signal probe1 (sP1) and signal probe2 (sP2). These probe structures were integrated into one DNA structure to develop the integrated signal probe (ISP) for multiple analyte detection [60]. In Figure 8, detection mechanism of ISP based aptasensor was presented. MB labeled hairpin DNA containing CEA-binding aptamer was used as sP1. Ferrocene (Fc)-modified MUC1-targeting aptamer as sP2 was designed as complementary to sP1. The hybridization between sP1 and sP2 **(Figure 8A)** was allowed to obtain ISP. Before immobilizing ISP to the bare glassy carbon electrodes, the surfaces were coated with AuNPs in order to advance sensitivity. Then, ISP was immobilized onto modified surfaces **(Figure 8B)** and formed to ISP/AuNPs/GCE. After having obtained ISP/AuNPs/GCE, MUC1 **(Figure 8C)** and CEA **(Figure 8D)** was sent to the sensing interface. sP1 unfolded after the binding to CEA and sP2 left from the ISP due to the formation of MUC1-aptamer complex. In the presence of CEA and MUC1 **(Figure 8E),** the current response of Fc and MB decreased due to the conformational change of aptamers, and thus, CEA and MUC1 can be simultaneously measured. LOD was determined as 0.5274 ng/mL for CEA and 1.82 nM for MUC1, respectively.

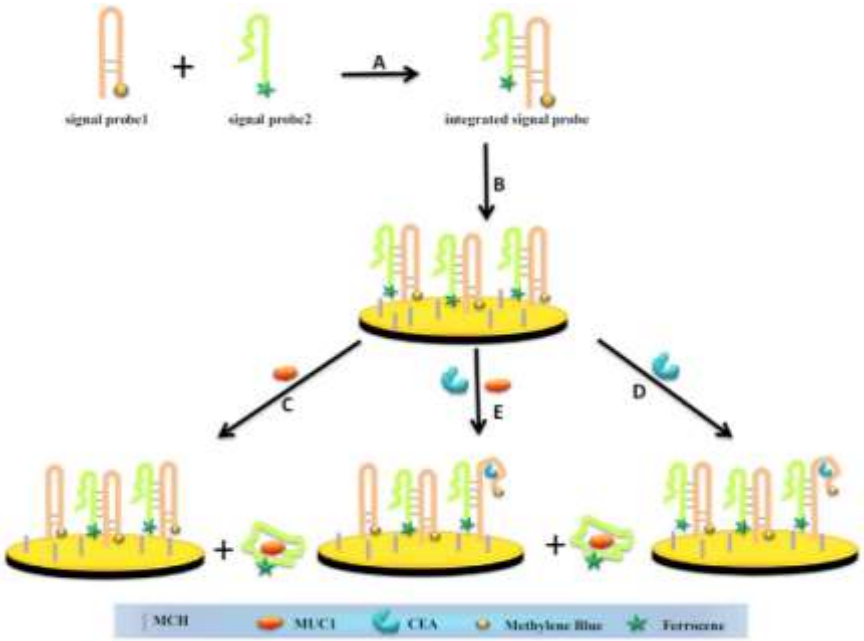

Figure 8: Schematic presentation of the ISP-based aptasensor for CEA and MUC-1 detection. (Reprinted from [60] with permission: ©2017 Elsevier B.V.).

As another example for dual cancer biomarker detection (CEA) and alpha-fetoprotein (AFP), a novel core-shell nanoparticle based structure was developed by using of different amounts of copper (Cu) and silver (Ag) precursors to increase the sensitivity and enhance the stability of AuNPs. The electrochemical detection was achieved with CV and DPV [61]. The experimental steps were presented in Figure 9. In this study, Au NPs core was used to accelerate the electron transfer. Two different core-shell nanoparticles were fabricated, involving Au@Cu_2O and Au@Ag as signal amplifiers. After producing Au@Cu_2O core-shell NPs and Au@Ag core-shell NPs, they were mixed with aptamer-C (aptamers against CEA) and aptamer-A (aptamers against AFP), respectively. Then, core-shell-aptamer were sent to the surface of aminated Probe A and Probe C immobilized GCE electrodes. The DPV peak currents was seen at −0.08 V for Au@Cu_2O core-shell NPs and at +0.26 V for Au@Ag core-shell NPs. The peaks at −0.08 V decreased with the increase of CEA concentration from 5 pg/ mL to 50 ng/mL. Meanwhile, the peaks at +0.26 V for Au@Ag NPs also decreased with AFP concentration from 1 pg/mL to 10 ng/mL as a proof of the specific interaction between the aptamers and analytes. LODs were determined as 1.8 pg/mL and 0.3 pg/mL for CEA and AFP, respectively.

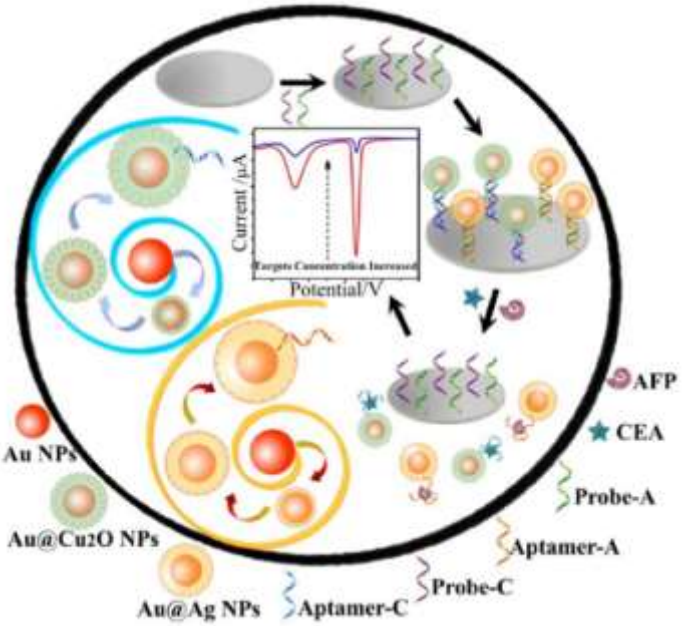

Figure 9: Schematic presentation of Au@Cu_2O core-shell NPs and Au@Ag core-shell NPs for specific CEA and AFP detection. (Reprinted from [61] with permission: ©2017 Elsevier B.V.).

3. APTASENSORS FOR SMALL MOLECULES DETECTION

In addition to electrochemical detection of biologically relevant analytes, aptamers could be also used to detect small molecules i.e., ligands, chemicals, toxins or drugs [62]. They also can easily conjugate to haptens, fluorophores, chromophores or enzymes for the interaction of small molecules. A novel aptamer-based impedimetric method was developed for detection of antifungal drug, carbendazim [63]. In this study, the aptamers were mounted onto the gold electrode surface and blocked with mercaptohexanol (MCH) to prevent unspecific binding.

As it was seen from Figure 10A, the bare electrode showed a reversible and higher signals. After the aptamer was sent to the surface, both the anodic and cathodic peak currents decreased. When the aptamer interacted with its target, the R_{ct} of the redox couple increased. Their results proved that the specific recognition of carbendazim with the thiol-modified aptamers. It also caused the alteration of the access of a ferrocyanide/ferricyanide to the surface (Figure 10B). EIS spectra of different concentrations of carbendazim was shown in Figure 10c. The calibration curve for carbendazim over CBZ concentration was shown in Figure 10D. The aptasensor did not show any cross reactivity with other pesticides. LOD was found as 8.2 pg/mL.

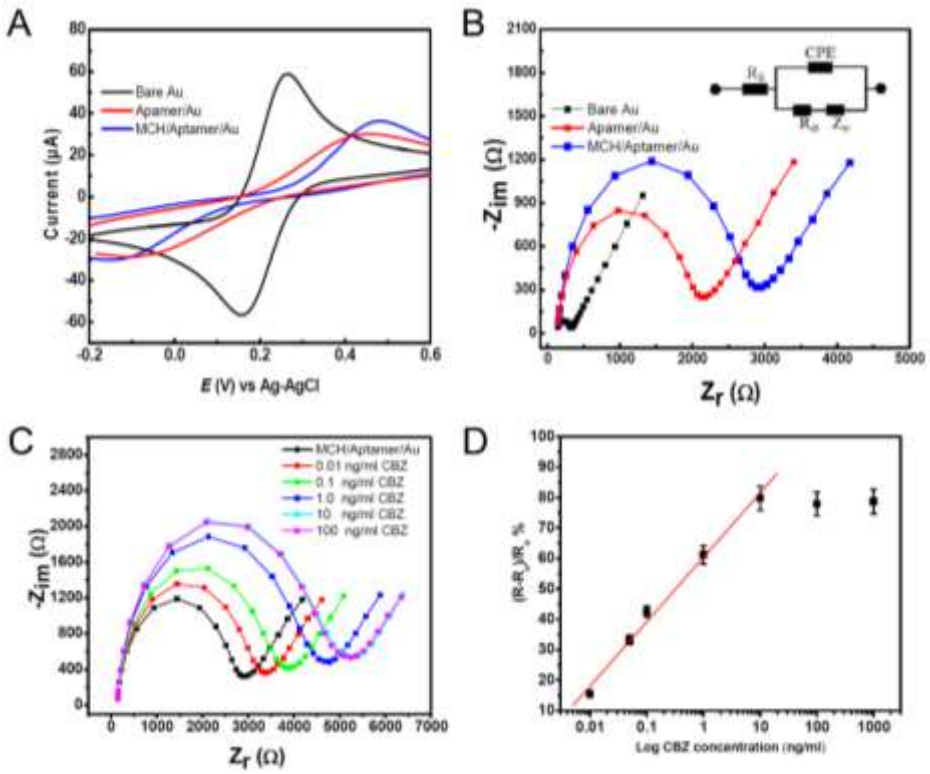

Figure 10: (A) CV curves and **(B)** Nyquist plots for bare electrode (black line), aptamer/Au (red line) and MCH/aptamer/Au (blue line) in $[Fe(CN)_6]^{3-/4-}$ solution. **(C)** Nyquist plots of aptasensor after incubation with 0, 0.01, 0.1, 1, 10 and 100 ng/ml of carbendazim. **(D)** The calibration curve for carbendazim (plot of $(R_o\text{-}R)/R_o$ % vs. logarithm of the CBZ concentration. (Reprinted from [63] with permission: ©2017 American Chemical Society).

In another study, MWCNTs and electropolymerized poly-L-glutamic acid based aptasensor for the determination of tetracycline was developed. Combining MWCNTs with polymers in the aptasensor construction improved the LOD. In addition, MWCNTs have larger surface in comparison with flat electrode. The reason of decreasing LOD was the immobilization of higher amount of biomolecules due to the increased binding sites on the electrodes. In this study, the sensor system was characterized with Scanning Electron Microscopy (SEM), CV and EIS. The aptasensor can be successfully used for the analysis of tetracycline in drug formulations and spiked honey samples [64].

Aptamers can be immobilized on a solid support, i.e., nano-structured surfaces. Binding properties of aptamers to their target molecules mostly depend on the proper 3-dimensional folding of aptamers. In addition, properties of nanostructured surfaces features (e.g. roughness, groves, pores) creates additional steric hindrance effects and thus, affect the interaction of aptamers with their targets. Therefore, it is extremely important to immobilize aptamers without affecting their binding ability into their targets. In recent years, combining nanomaterials such as nanoparticles, nanotubes, nanorods, fibers with polymers has been taking significant attention as they provide a proper surface, e.g., high area of interaction between aptamer and target analyte. Especially, AuNPs are very promising thanks to their extraordinary properties, such as long term stability and biological compatibility, tunable morphology and size dispersion and easy surface functionalization. Moreover, interaction of thiols with gold is a well-known and described mechanism resulting in formation of stable self-assembled monolayers (SAM) which enables to design stable aptasensor systems. The use of gold nanoparticles also enhances the signals dramatically because of the localized surface plasmons excited on the surface and the formation of a target-analyte complex enabling charge transfers [65].

Sensitive detection and quantitation of antibiotic residues in real samples are in great demand. Yu et al. developed a broad-spectrum antibiotic aptasensor in serum, saliva, and milk with ACV [66]. As an antibiotic, they used ampicillin. The aptasensor was based on signal-ON principle in which the target binding-induced changes in the conformation of aptamer. When MB modified aptamer was introduced with ampicillin, the aptamer structure either unstructured or partially folded. In the presence of target, the electron transfer between MB label and the gold electrode changed due to probe conformation and flexibility. The change in the probe conformation produced an increase in the MB current, resulting in a signal-ON sensor behavior. In this study, authors could successfully achieve to differentiate between ampicillin and amoxicillin, which is structurally similar to antibiotic. The method was selective to be used without any pretreatment in complex samples with 1 µM of LOD.

In other study, Fan et al. showed detection of acetamiprid with EIS by using AuNPs to improve the sensitivity [67]. First, they immobilized AuNPs onto the electrode surface, then the analyte were sent to the modified surface. In the presence of analyte, the electron transfer resistance increased due to the formation of aptamer/target couple. In a very similar study, Fei et al. improved the sensitivity by using AuNPs combined with MWCNT-reduced graphene oxide nanoribbon composites [68]. The designed impedimetric based aptasensor was successfully employed to identify acetamiprid in water in femtomole level.

Recently, researchers aimed to develop a label-free aptasensor to detect a natural and toxic mycotoxin, Aflatoxin B, by using a reduced graphene oxide/molybdenum disulfide/polyaniline nanocomposite/gold nanoparticles (RGO/MoS_2/PANI@AuNPs/Apt) [69]. The developed nanocomposites were characterized by UV-visible Spectroscopy, Fourier Transform Infrared Spectroscopy (FTIR), Transmission Electron Microscopy (TEM) and X-Ray Photoelectron Spectroscopy (XPS). The GCE was coated with chitosan (Cs) to improve rigidity and stability of aptasensor as chitosan provided excellent film-forming ability and good adhesion.

The Cs/RGO/MoS_2/PANI coated electrodes were then immersed into AuNPs solution for 12 hours. Subsequently, Cs/RGO/MoS_2/PANI@AuNPs electrodes were incubated with aptamer solution for another 12 hours. Then, the electrodes were immersed into mercaptohexanol solution for 2 h to block the excessively activate sites. Finally, the developed aptasensor was rinsed, dried and used directly or stored dry at 4 °C. In the presence of Aflatoxin B1 resulted in the reduction of electron transfer of $[Fe(CN)_6]^{3-/4-}$. The signal differences were measured with DPV. Taking advantages of RGO/MoS_2/PANI/Cs composites and AuNPs signal amplification, the electrochemical aptasensor showed a low LOD of 0.002 fg/mL and wide linear range, 0.01 fg/mL to 1.0 fg/mL.

Wang et al. developed an aptasensor to detect aflatoxin B1 (AFB1), which have mutagenic, teratogenic and carcinogenic effects [70]. First, anti-AFB1 thiolated tagged aptamer, which contained MB label, was immobilized onto the gold electrode. In the absence of analyte, complementary DNA strand of aptamer hybridized with aptamer to form a rigid duplex DNA structure, leading a lower current. In the presence of analyte, the current increased due to the aptamer-AFB1 binding that caused the formation of a hairpin structure making MB close to electrode. LOD was found as 2 nM. The most attractive feature of the designed aptasensor was that it only requires 5-min incubation of sample solution before SWV analysis.

One of the most used antibiotic, kanamycin are generally preferred in food production and livestock husbandry and the detection of the kanamycin as residue in food samples within this range is quite essential. A recent study tried to detect kanamycin in milk samples by using an ultrasensitive and simple aptasensor with chemiluminescence (ECL) properties of luminol-H_2O_2 in alkaline solution with CV and electrogenerated chemiluminescence analyzer [71]. Silver nanoparticles (AgNPs) were used as effective catalyzer to accelerate H_2O_2 decomposition to produce various reactive oxygen species for signal amplification. The luminescence reagent, co-reactant and AgNPs were immobilized onto the platinium electrode (PE) surface. The steps for detection of kanamycin was presented in Figure 11. LOD was calculated as 0.06 ng/ mL with a wide linear range from 0.5 to 100 ng/mL.

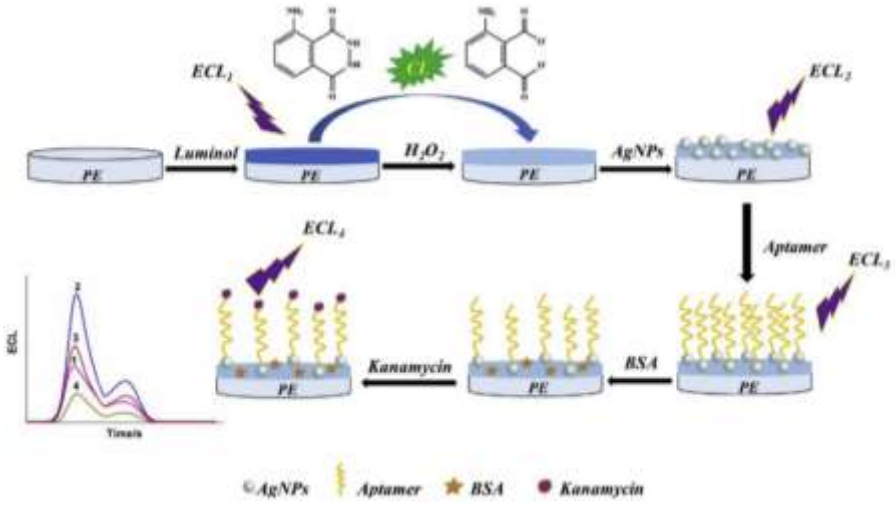

Figure 11: Schematic of the aptasensor for the detection of kanamycin (BSA: Bovine Serum Albumin). (Reprinted from [71] with permission: ©2019 Elsevier B.V. All rights reserved.).

Some of aptasensor examples for small molecule detection are listed in Table 3.

Table 3: Electrochemical-based aptasensors for different types of small molecule detection and their respective sensitivities.

METHOD	ANALYTE	TARGET	LOD	REFERENCE
EIS	Doxorubicin	Drug	28 nM	[72]
EIS, CV	Kanamycin	Drug	0.11 ng/mL	[73]
EIS	Chloramphenicol	Drug	57.9 pM	[74]
EIS	Codeine	Drug	3 pM	[75]
EIS	Carbendazim	Drug	8.2 pg/mL	[76]
SWV	Dabigatran etexilate	Drug	0. 01ng/ml	[77]
EIS	Diclofenac	Drug	2.7 nM	[78]
EIS	Dexamethasone	Drug	2.12 nM	[79]
EIS	Tobramycin	Drug	2.0 fg/mL	[80]
DPV	Oxaliplatin	Drug	60 pmol/L	[81]
EIS, CV, DPV	Chloramphenicol	Drug	3.3 pM	[82]
EIS, CV	Aflatoxin M1	Toxin	5 ng/L	[83]
EIS	Okadaic acid	Toxin	70 pg/mL	[84]
EIS, CV	Natoxin-a	Toxin	0.5 nM	[85]
Amperometry	Toxin A	Toxin	1 nM	[86]
DPV, CV, EIS	Malachite green	Chemical	3.38 nM	[87]
DPV, CV	Ractopamine	Chemical	5.0×10^{-13} M	[88]
Potentiometry	Bisphenol A	Chemical	10^{-8} M	[89]
DPV	Cocaine	Chemical	0.5 pM	[90]
EIS	Ethanolamine	Chemical	0.08 nM	[91]
CV, DPV	Malathion	Chemical	0.5 fM	[92]
SWV	Beta-lactoglobulin	Allergen	20 pg/ml	[93]

Abbreviations: LOD: Limit of Detection; **EIS:** Electrochemical Impedance Spectroscopy; **CV:** Cyclic Voltammetry; **DPV:** Differential Pulse Voltammetry; **SWV:** Square Wave Voltammetry.

An impedimetric aptasensor was developed with affinity chromatography and EIS for detection of penicillin G in milk samples [94]. Capture-SELEX, a suitable method for developing aptamer against small molecules like antibiotics, was used to select best aptamer candidate among the 11 candidate aptamers. The developed method was based on the selection of DNA aptamers using penicillin in solution while the ssDNA library is fixed on a support. Then, the ssDNA linked to the target were directly amplified by PCR. Capture-SELEX enabled to avoid target immobilization, which often hampered appropriate interactions with oligonucleotides. Using Capture-SELEX method, penicillin G was successfully detected with an LOD of 0.17 µg/L, which is lower than ELISA methods (3 µg/L).

Researchers introduced a potentiometric aptasensor platform that combines G-quadruplex/hemin DNAzyme with logic gate operations for Kanamycin (KANA) and oxytetracycline (OTC) detection using a single membrane electrode [95]. In the system, DNAzymes can be incorporated into an aptamer binding event that eliminates the need for probe labeling. A polymeric membrane ion-selective electrode is used in potentiometry that could be derived to a simple and portable electrochemical detection method. The system could be also used for the detection of multiples analytes by changing the target aptamers in the probe sequences.

Heavy metal ions such as Hg^{2+}, Pb^{2+}, Cd^{2+}, $Sb3^{+}$ and As^{3+} are toxic ions and can be harmful for both human health and the ecosystem. For the detection of heavy metals, rapid, cost-effective and easy applicable alternative analysis methods for heavy metal ions are desired. In this regard, electrochemical based aptasensors are very promising for sensitive, specific and accurate detection of heavy metals. For a highly sensitive detection of Pb^{2+}, Gao et al. developed a label-free electrochemical aptasensor by combining and graphene with CV. In the study, thionine was used as signaling molecule and graphene as a signal-enhancer. After the interaction with Pb^{2+}, aptamer on the sensor surface changed its conformation from a single-stranded DNA to a G-quadruplex that causes thionine release from the electrode surface into the solution and resulted a decrease of the signal belongs to thionine. The redox signal obtained from CV was significantly lower in graphene assembled electrode than the bare one, which showed that graphene played an important role in the electrochemical response of the sensor. LOD was found as 3.2×10^{-14} M [96]. Compared to the electrochemical systems with classical methods, e.g., Inductively Coupled Plasma Mass Spectroscopy (ICP-MS), Atomic Absorption Spectroscopy, (AAS), and High Performance Liquid Chromatography (HPLC) for heavy metals ions detection, electrochemical based systems have several advantages such as offering low cost instrumentation and low-cost. Furthermore, classical methods have multiple pre-steps, which results in longer experimental duration.

5. SUMMARY

Aptamers are an alternative diagnostic tool that can substitute antibodies in various applications, i.e., detecting specific biomarkers, cells or proteins. Not limited to biological molecules, chemical ligands, such as toxins or drugs, can be targeted with aptamers. Aptamers can be combined with a wide range of transduction forms, e.g., electrochemical, optical, thermal

or mass sensitive. Among these forms, electrochemical methods are mostly preferred due to their ability to provide rapid response, low cost analysis, easy of application and selective detection. A significant number of voltammetric, amperometric, potentiometric and impedimetric based electrochemical aptasensors have been developed for the detection of biological molecules or synthetic chemicals. Among these electrochemical aptasensors, amperometric and impedimetric measurements are the most preferred ones compared to the other electrochemical methods. Up to now, researchers have used unique properties of nanomaterials to optimize different aptasensors. The use of biosensors, providing enhanced surface area for immobilization or conjugation of biological analytes or small molecules, led to an improvement in the sensitivity and efficiency of these aptasensors.

There are still plenty of nanomaterials need to be tested for the enhancing the analytical signals of the developed aptasensors systems. Lower detection limits up to sub- femtomolar/attomolar levels and wide linear analytical ranges are urgently needed with the help of nanomaterials, nanocomposites, or their combinations. More importantly, when developing aptansensor based detection systems with electrochemical transducers, it is critical to consider the simultaneous detection of analytes and stability of biosensor assays. Integration of point-of-care devices for analyte detection should be widely distributed in the market. Despite the presence of very successful aptamers developed in laboratory infrastructure, there are still very few aptamers approved in the clinical applications. Although aptamers possess more advantages compared to antibodies, antibodies are still being more frequently used compared to aptamers as of now. With this in mind, in the near future, aptamers could be the key player for the detection of biologically important molecules.

FIGURE LEGENDS

Figure 1: (A) The steps for general SELEX process: binding, partitioning and amplification (Reprinted from [13] with permission: ©2017 MDPI AG). **(B)** Cell-SELEX process (Reprinted from [14] with permission: ©2017 MDPI AG).

Figure 2: (A) Presentation of isolation and determination of HL-60 cells using aptamer-modified self-propelled nanomotors **(**Reprinted from [28] with permission: ©2018 Elsevier B.V.). **(B)** Presentation of fabrication of sandwich-type aptasensor (Reprinted from [29] with permission: ©2017 Elsevier B.V.).

Figure 3: (A) Schematic presentation of detection of PSA biomarker by using an electrochemical system **(B)** EIS spectra of bare and different modified electrodes in 5.0 mM $[Fe(CN)_6]^{3-/4-}$ (Reprinted from [31] with permission: ©2019 Elsevier B.V.).

Figure 4: (A) Schematic presentation of TLS11a aptamer and its interaction with HepG2 cells. **(B)** CV and **(C)** Nyquist plots for (a) bare GE, (b) GE/MPA, (c) GE/MPA/APT (d) GE/MPA/APT/HepG2 cell, (e) GE/MPA/APT/HepG2/APT **(D)** Nyquist plots in the same conditions of A and B, (a−i) GE/MPA/APT/cell/APT (0, 10, 10^2, 10^3, 10^4, 10^5, 5×10^5, 10^6 and $1.5x10^6$ HepG2 cells/mL). **(E)** Calibration plots for the developed aptasensor (Reprinted from [33] with permission: ©2014 American Chemical Society).

Figure 5: (A) Schematic presentation of an aptasensor to detect EpCAM molecule via DNA recycling amplification **(B)** Current signals obtained from different concentrations of EpCAM in the presence of EpCAM aptamer/probe A and Hp2 (from bottom to top: 0 to 300 ng/mL) by using SWV measurements. **(C)** Calibration curve of different concentrations of EpCAM. (Hp1: Hairpin probe 1; Hp2: Hairpin probe 2; MB: Methylene blue; MCH: 6-Mercapto-1-hexanol; EpCAM: Epithelial cell adhesion molecule). (Reprinted from [37] with permission: ©2020 Springer Nature Switzerland AG.).

Figure 6: The main principle of the (A) signal-ON and (B) signal-OFF strategy in electrochemical aptasensors (Reprinted from [38] with permission: ©2020 Springer Nature Switzerland AG.).

Figure 7: Schematic representation of the Janus nanoparticles-based detection for CEA biomarker by using NCR-80 and OHT-000) (Reprinted from [39] with permission: ©2019 Elsevier B.V.).

Figure 8: Schematic presentation of the ISP-based aptasensor for CEA and MUC-1 detection. (Reprinted from [60] with permission: ©2017 Elsevier B.V.).

Figure 9: Schematic presentation of Au@Cu_2O core-shell NPs and Au@Ag core-shell NPs for specific CEA and AFP detection. (Reprinted from [61] with permission: ©2017 Elsevier B.V.).

Figure 10: (A) CV curves and **(B)** Nyquist plots for bare electrode (black line), aptamer/Au (red line) and MCH/aptamer/Au (blue line) in $[Fe(CN)_6]^{3-/4-}$ solution. **(C)** Nyquist plots of aptasensor after incubation with 0, 0.01, 0.1, 1, 10 and 100 ng/ml of carbendazim. **(D)** The calibration curve for carbendazim (plot of $(R_o-R)/R_o$ % vs. logarithm of the CBZ concentration. (Reprinted from [63] with permission: ©2017 American Chemical Society).

Figure 11: Schematic of the aptasensor for the detection of kanamycin (BSA: Bovine Serum Albumin). (Reprinted from [71] with permission: ©2019 Elsevier B.V. All rights reserved.).

Table 1: Comparison of aptamers and antibodies in terms of target type, synthesis time, stability, size, chemical modification, production, cost and toxicity.

Table 2: Electrochemical based aptasensors for detecting different types of biological analytes and their respective sensitivities.

Table 3: Electrochemical-based aptasensors for different types of small molecule detection and their respective sensitivities.

DATA AVAILABILITY STATEMENT

Data sharing is not applicable to this article as no new data were created or analyzed in this study.

CONFLICT OF INTEREST

The authors declare that there is no conflict of interests regarding the publication of this paper.

REFERENCES

[1] L. C. Bock, L. C. Griffin, J. A. Latham, E. H. Vermaas, J. J. Toole, *Nature* **1992**, *355*, 564-566.

[2] G. Mayer, *Angew Chem Int Edit* **2009**, *48*, 2672-2689.

[3] A. Ozer, J. M. Pagano, J. T. Lis, *Molecular therapy. Nucleic acids* **2014**, *3*, e183.

[4] G. C. Pugh, J. R. Burns, S. Howorka, *Nat Rev Chem* **2018**, *2*, 113-130.

[5] M. Ilgu, M. Nilsen-Hamilton, *The Analyst* **2016**, *141*, 1551-1568.

[6] A. D. Ellington, J. W. Szostak, *Nature* **1990**, *346*, 818-822.

[7] aN. Duan, W. Gong, S. Wu, Z. Wang, *Analytica chimica acta* **2017**, *961*, 100-105; bH. Hasegawa, N. Savory, K. Abe, K. Ikebukuro, *Molecules* **2016**, *21*, 421; cK. Yarizadeh, M. Behbahani, H. Mohabatkar, A. Noorbakhsh, *Journal of biotechnology* **2019**.

[8] A. Boussebayle, D. Torka, S. Ollivaud, J. Braun, C. Bofill-Bosch, M. Dombrowski, F. Groher, K. Hamacher, B. Suess, *Nucleic acids research* **2019**, *47*, 4883-4895.

[9] K. Pleiko, L. Saulite, V. Parfejevs, K. Miculis, E. Vjaters, U. Riekstina, *Scientific reports* **2019**, *9*, 8142.

[10] X. J. Yang, H. Zhu, S. R. Mu, W. J. Wei, X. Yuan, M. Wang, Y. Liu, J. Hui, Y. Huang, *The Journal of biological chemistry* **2019**, *294*, 10998-11010.

[11] L. Dong, Q. Tan, W. Ye, D. Liu, H. Chen, H. Hu, D. Wen, Y. Liu, Y. Cao, J. Kang, J. Fan, W. Guo, W. Wu, *Scientific reports* **2015**, *5*, 15552.

[12] aA. Sinha, P. Gopinathan, Y. D. Chung, H. Y. Lin, K. H. Li, H. P. Ma, P. C. Huang, S. C. Shiesh, G. B. Lee, *Biosensors & bioelectronics* **2018**, *122*, 104-112; bK. M. Ahmad, S. S. Oh, S. Kim, F. M. McClellen, Y. Xiao, H. T. Soh, *PloS one* **2011**, *6*, e27051.

[13] S. Catuogno, C. L. Esposito, *Biomedicines* **2017**, *5*.

[14] E. M. Hays, W. Duan, S. Shigdar, *International journal of molecular sciences* **2017**, *18*.

[15] aB. H. Lee, S. H. Kim, Y. Ko, J. C. Park, S. Ji, M. B. Gu, *Biosensors & bioelectronics* **2019**, *126*, 122-128; bH. A. Alhadrami, R. Chinnappan, S. Eissa, A. A. Rahamn, M. Zourob, *Analytical biochemistry* **2017**, *525*, 78-84; cK. Abe, W. Yoshida, K. Ikebukuro, *Adv Biochem Eng Biot* **2014**, *140*, 183-202; dK. Sefah, J. A. Phillips, X. Xiong, L. Meng, D. Van Simaeys, H. Chen, J. Martin, W. Tan, *The Analyst* **2009**, *134*, 1765-1775.

[16] C. K. O'Sullivan, *Anal Bioanal Chem* **2002**, *372*, 44-48.

[17] aN. Reta, C. P. Saint, A. Michelmore, B. Prieto-Simon, N. H. Voelcker, *ACS applied materials & interfaces* **2018**, *10*, 6055-6072; bN. F. D. Silva, J. Magalhaes, C. Freire, C. Delerue-Matos, *Biosensors & bioelectronics* **2018**, *99*, 667-682; cM. Sanchez-Paniagua Lopez, E. Redondo-Gomez, B. Lopez-Ruiz, *Talanta* **2017**, *175*, 209-216; dP. Panjan, V. Virtanen, A. M. Sesay, *Talanta* **2017**, *170*, 331-336; eS. Campuzano, P. Yanez-Sedeno, J. M. Pingarron, *Diagnostics* **2016**, *7*; fS. N. Topkaya, V. H. Ozyurt, A. E. Cetin, S. Otles, *Biosensors & bioelectronics* **2018**, *102*, 464-469; gS. N. Topkaya, *Biosensors & bioelectronics* **2015**, *64*, 456-461; hS. N. Topkaya, B. Kosova, M. Ozsoz, *Clinica chimica acta; international journal of clinical chemistry* **2014**, *429*, 134-139; iS. N. Topkaya,

S. Aydinlik, N. Aladag, M. Ozsoz, D. Ozkan-Ariksoysal, *Combinatorial chemistry & high throughput screening* **2010**, *13*, 582-589.

[18] D. Grieshaber, R. MacKenzie, J. Voros, E. Reimhult, *Sensors-Basel* **2008**, *8*, 1400-1458.

[19] aM. Ganesana, E. Trikantzopoulos, Y. Maniar, S. T. Lee, B. J. Venton, *Biosensors & bioelectronics* **2019**, *130*, 103-109; bA. Ivanov, R. Davletshina, I. Sharafieva, G. Evtugyn, *Talanta* **2019**, *194*, 723-730; cM. Cerrato-Alvarez, E. Bernalte, M. J. Bernalte-Garcia, E. Pinilla-Gil, *Talanta* **2019**, *193*, 93-99.

[20] aS. Kumar, S. Panwar, S. Kumar, S. Augustine, B. D. Malhotra, *Nanomaterials* **2019**, *9*; bX. Wang, M. Yang, Q. Liu, S. Yang, X. Geng, Y. Yang, H. Fa, Y. Wang, C. Hou, *Analytical sciences : the international journal of the Japan Society for Analytical Chemistry* **2019**, *35*, 441-448; cI. Rassas, M. Braiek, A. Bonhomme, F. Bessueille, G. Rafin, H. Majdoub, N. Jaffrezic-Renault, *Materials science & engineering. C, Materials for biological applications* **2019**, *95*, 152-159; dA. Beheshti-Marnani, A. Hatefi-Mehrjardi, Z. Es'haghi, *Colloids and surfaces. B, Biointerfaces* **2019**, *175*, 98-105; eM. Zhong, L. Yang, H. Yang, C. Cheng, W. Deng, Y. Tan, Q. Xie, S. Yao, *Biosensors & bioelectronics* **2019**, *126*, 493-500.

[21] aT. A. R. Cordeiro, M. V. C. Goncalves, D. L. Franco, A. B. Reis, H. R. Martins, L. F. Ferreira, *Talanta* **2019**, *195*, 327-332; bY. Ye, J. Ji, F. Pi, H. Yang, J. Liu, Y. Zhang, S. Xia, J. Wang, D. Xu, X. Sun, *Biosensors & bioelectronics* **2018**, *119*, 119-125; cM. Srivastava, N. R. Nirala, S. K. Srivastava, R. Prakash, *Scientific reports* **2018**, *8*, 1923.

[22] K. Sun, N. Xia, L. J. Zhao, K. Liu, W. J. Hou, L. Liu, *Sensor Actuat B-Chem* **2017**, *245*, 87-94.

[23] P. Jolly, A. Miodek, D. K. Yang, L. C. Chen, M. D. Lloyd, P. Estrela, *Acs Sensors* **2016**, *1*, 1308-1314.

[24] Y. Zhao, Y. X. Yang, Y. L. Sun, L. Y. Cui, F. J. Zheng, J. R. Zhang, Q. J. Song, C. L. Xu, *Biosensors & bioelectronics* **2018**, *99*, 193-200.

[25] M. A. H. Nawaz, S. Rauf, G. Catanante, M. H. Nawaz, G. Nunes, J. L. Marty, A. Hayat, *Sensors-Basel* **2016**, *16*.

[26] W. Li, Z. Nie, X. H. Xu, Q. P. Shen, C. Y. Deng, J. H. Chen, S. Z. Yao, *Talanta* **2009**, *78*, 954-958.

[27] H. L. Dong, H. F. Chen, J. Q. Jiang, H. Zhang, C. X. Cai, Q. M. Shen, *Anal Chem* **2018**, *90*, 4507-4513.

[28] M. Amouzadeh Tabrizi, M. Shamsipur, R. Saber, S. Sarkar, *Biosensors & bioelectronics* **2018**, *110*, 141-146.

[29] M. Amouzadeh Tabrizi, M. Shamsipur, R. Saber, S. Sarkar, *Analytica chimica acta* **2017**, *985*, 61-68.

[30] B. P. Crulhas, A. E. Karpik, F. K. Delella, G. R. Castro, V. A. Pedrosa, *Anal Bioanal Chem* **2017**, *409*, 6771-6780.

[31] Z. J. Li, J. F. Yin, C. H. Gao, G. H. Qiu, A. A. Meng, Q. D. Li, *Sensor Actuat B-Chem* **2019**, *295*, 93-100.

[32] M. Jarczewska, R. Ziolkowski, L. Gorski, E. Malinowska, *Electroanal* **2018**, *30*, 658-664.

[33] L. Kashefi-Kheyrabadi, M. A. Mehrgardi, E. Wiechec, A. P. F. Turner, A. Tiwari, *Anal Chem* **2014**, *86*, 4956-4960.

[34] Y. Zhao, L. Cui, Y. Sun, F. Zheng, W. Ke, *ACS applied materials & interfaces* **2019**, *11*, 3474-3481.

[35] X. Y. Liu, K. Q. Deng, H. Wang, C. X. Li, S. W. Zhang, H. W. Huang, *Microchim Acta* **2019**, *186*.

[36] B. H. Lee, S. H. Kim, Y. Ko, J. C. Park, S. Ji, M. B. Gu, *Biosens Bioelectron* **2019**, *126*, 122-128.

[37] Q. Chen, W. Hu, B. Shang, J. Wei, L. Chen, X. Guo, F. Ran, W. Chen, X. Ding, Y. Xu, Y. Wu, *Mikrochimica acta* **2018**, *185*, 202.

[38] A. Villalonga, A. M. Perez-Calabuig, R. Villalonga, *Anal Bioanal Chem* **2020**, *412*, 55-72.

[39] G. Paniagua, A. Villalonga, M. Eguilaz, B. Vegas, C. Parrado, G. Rivas, P. Diez, R. Villalonga, *Analytica chimica acta* **2019**, *1061*, 84-91.

[40] J. Cao, X. P. Zhao, M. R. Younis, Z. Q. Li, X. H. Xia, C. Wang, *Anal Chem* **2017**, *89*, 10957-10964.

[41] T. S. Wang, J. Y. Liu, X. X. Gu, D. Li, J. Wang, E. Wang, *Analytica chimica acta* **2015**, *882*, 32-37.

[42] C. Y. Lu, J. J. Xu, Z. H. Wang, H. Y. Chen, *Electrochem Commun* **2015**, *52*, 49-52.

[43] X. J. Chen, Y. Z. Wang, Y. Y. Zhang, Z. H. Chen, Y. Liu, Z. L. Li, J. H. Li, *Anal Chem* **2014**, *86*, 4278-4286.

[44] K. Wang, M. Q. He, F. H. Zhai, R. H. He, Y. L. Yu, *Talanta* **2017**, *166*, 87-92.

[45] N. Zhou, F. Su, Z. Li, X. Yan, C. Zhang, B. Hu, L. He, M. Wang, Z. Zhang, *Mikrochimica acta* **2019**, *186*, 75.

[46] E. Heydari-Bafrooei, N. S. Shamszadeh, *Biosensors & bioelectronics* **2017**, *91*, 284-292.

[47] H. Ilkhani, M. Sarparast, A. Noori, S. Z. Bathaie, M. F. Mousavi, *Biosensors & bioelectronics* **2015**, *74*, 491-497.

[48] B. Kavosi, A. Salimi, R. Hallaj, F. Moradi, *Biosensors & bioelectronics* **2015**, *74*, 915-923.

[49] A. Salek Maghsoudi, S. Hassani, M. Rezaei Akmal, M. R. Ganjali, K. Mirnia, P. Norouzi, M. Abdollahi, *International journal of nanomedicine* **2020**, *15*, 2219-2230.

[50] Z. Taleat, C. Cristea, G. Marrazza, M. Mazloum-Ardakani, R. Sandulescu, *J Electroanal Chem* **2014**, *717*, 119-124.

[51] X. J. Qiao, K. X. Li, J. Q. Xu, N. Cheng, Q. L. Sheng, W. Cao, T. L. Yue, J. B. Zheng, *Biosensors & bioelectronics* **2018**, *113*, 142-147.

[52] D. Sun, Z. Luo, J. Lu, S. Zhang, T. Che, Z. Chen, L. Zhang, *Biosensors & bioelectronics* **2019**, *134*, 49-56.

[53] M. Tertis, B. Ciui, M. Suciu, R. Sandulescu, C. Cristea, *Electrochim Acta* **2017**, *258*, 1208-1218.

[54] I. Letchumanan, S. C. B. Gopinath, M. K. Md Arshad, P. Anbu, T. Lakshmipriya, *Biosensors & bioelectronics* **2019**, *131*, 128-135.

[55] X. Y. Huang, B. B. Cui, Y. S. Ma, X. Yan, L. Xia, N. Zhou, M. H. Wang, L. H. He, Z. H. Zhang, *Analytica chimica acta* **2019**, *1078*, 125-134.

[56] A. Gosai, B. S. Hau Yeah, M. Nilsen-Hamilton, P. Shrotriya, *Biosensors & bioelectronics* **2019**, *126*, 88-95.

[57] M. Amouzadeh Tabrizi, M. Shamsipur, R. Saber, S. Sarkar, M. Besharati, *Mikrochimica acta* **2017**, *185*, 59.

[58] S. Y. Park, J. Kim, G. Yim, H. Jang, Y. Lee, S. M. Kim, C. Park, M. H. Lee, T. Lee, *Colloids and surfaces. B, Biointerfaces* **2020**, *195*, 111240.

[59] H. A. Samie, M. Arvand, *Bioelectrochemistry* **2020**, *133*, 107489.

[60] J. Xiang, X. Pi, X. Chen, L. Xiang, M. Yang, H. Ren, X. Shen, N. Qi, C. Deng, *Biosensors & bioelectronics* **2017**, *96*, 268-274.

[61] Y. Zhao, Y. Yang, Y. Sun, L. Cui, F. Zheng, J. Zhang, Q. Song, C. Xu, *Biosensors & bioelectronics* **2018**, *99*, 193-200.

[62] aY. X. Zhang, J. F. Xia, F. F. Zhang, Z. H. Wang, Q. Y. Liu, *Sensor Actuat B-Chem* **2018**, *267*, 412-418; bK. Abnous, N. M. Danesh, M. Ramezani, S. M. Taghdisi, A. S. Emrani, *Anal Methods-Uk* **2018**, *10*, 3232-3236; cA. Azadbakht, S. Beirnvand, *Microchim Acta* **2017**, *184*, 2825-2835.

[63] S. Eissa, M. Zourob, *Anal Chem* **2017**, *89*, 3138-3145.

[64] A. Benvidi, S. Yazdanparast, M. Rezaeinasab, M. D. Tezerjani, S. Abbasi, *J Electroanal Chem* **2018**, *808*, 311-320.

[65] G. Q. Wang, Y. Q. Wang, L. X. Chen, J. Choo, *Biosensors & bioelectronics* **2010**, *25*, 1859-1868.

[66] Z. G. Yu, R. Y. Lai, *Talanta* **2018**, *176*, 619-624.

[67] L. Fan, G. Zhao, H. Shi, M. Liu, Z. Li, *Biosensors & bioelectronics* **2013**, *43*, 12-18.

[68] A. Fei, Q. Liu, J. Huan, J. Qian, X. Dong, B. Qiu, H. Mao, K. Wang, *Biosensors & bioelectronics* **2015**, *70*, 122-129.

[69] G. S. Geleta, Z. Zhao, Z. X. Wang, *The Analyst* **2018**, *143*, 1644-1649.

[70] C. Wang, Y. P. Li, Q. Zhao, *Biosensors & bioelectronics* **2019**, *144*.

[71] S. T. Cheng, H. M. Liu, H. Zhang, G. L. Chu, Y. M. Guo, X. Sun, *Sensor Actuat B-Chem* **2020**, *304*.

[72] N. Bahner, P. Reich, D. Frense, M. Menger, K. Schieke, D. Beckmann, *Anal Bioanal Chem* **2018**, *410*, 1453-1462.

[73] A. Sharma, G. Istamboulie, A. Hayat, G. Catanante, S. Bhand, J. L. Marty, *Sensor Actuat B-Chem* **2017**, *245*, 507-515.

[74] X. Qin, Q. Wang, L. Geng, X. Shu, Y. Wang, *Talanta* **2019**, *197*, 28-35.

[75] L. Huang, X. Yang, C. Qi, X. Niu, C. Zhao, X. Zhao, D. Shangguan, Y. Yang, *Analytica chimica acta* **2013**, *787*, 203-210.

[76] S. Eissa, M. Zourob, *Analytical chemistry* **2017**, *89*, 3138-3145.

[77] M. M. Aljohani, R. Chinnappan, S. Eissa, O. A. Alsager, K. Weber, D. Cialla-May, J. Popp, M. Zourob, *Scientific reports* **2018**, *8*, 13290.

[78] H. Derikvand, M. Roushani, A. R. Abbasi, Z. Derikvand, A. Azadbakht, *Analytical biochemistry* **2016**, *513*, 77-86.

[79] S. Mehennaoui, S. Poorahong, G. C. Jimenez, M. Siaj, *Scientific reports* **2019**, *9*, 6600.

[80] S. J. Wang, Z. Z. Li, F. H. Duan, B. Hu, L. H. He, M. H. Wang, N. Zhou, Q. J. Jia, Z. H. Zhang, *Analytica chimica acta* **2019**, *1047*, 150-162.

[81] M. M. El-Wekil, M. Darweesh, M. S. A. Shaykoon, R. Ali, *Talanta* **2020**, *217*, 121084.

[82] M. Roushani, Z. Rahmati, S. Farokhi, S. J. Hoseini, R. H. Fath, *Materials science & engineering. C, Materials for biological applications* **2020**, *108*, 110388.

[83] V. Stepanova, V. Smolko, V. Gorbatchuk, I. Stoikov, G. Evtugyn, T. Hianik, *Sensors-Basel* **2019**, *19*.

[84] S. Eissa, A. Ng, M. Siaj, A. C. Tavares, M. Zourob, *Anal Chem* **2013**, *85*, 11794-11801.

[85] R. Elshafey, M. Siaj, M. Zourob, *Biosensors & bioelectronics* **2015**, *68*, 295-302.

[86] P. Luo, Y. Liu, Y. Xia, H. Xu, G. Xie, *Biosensors & bioelectronics* **2014**, *54*, 217-221.

[87] Q. Wang, X. Qin, L. Geng, Y. Wang, *Nanomaterials* **2019**, *9*.

[88] F. Yang, P. Wang, R. Wang, Y. Zhou, X. Su, Y. He, L. Shi, D. Yao, *Biosensors & bioelectronics* **2016**, *77*, 347-352.

[89] E. G. Lv, J. W. Ding, W. Qin, *Sensor Actuat B-Chem* **2018**, *259*, 463-466.

[90] M. Roushani, F. Shahdost-Fard, *Materials science & engineering. C, Materials for biological applications* **2016**, *61*, 599-607.

[91] G. Liang, Y. Man, X. Jin, L. Pan, X. Liu, *Analytica chimica acta* **2016**, *936*, 222-228.

[92] N. Kaur, H. Thakur, N. Prabhakar, *Microchem J* **2019**, *147*, 393-402.

[93] S. Eissa, M. Zourob, *Biosensors & bioelectronics* **2017**, *91*, 169-174.

[94] N. P. G. Istamboulie, A. Triki, C. Lozano, L. Barthelmebs, T. Noguer, *Talanta* **2017**, *162*, 232-240.

[95] S. Liu, J. Ding, W. Qin, *Anal Chem* **2019**, *91*, 3170-3176.

10.1002/elan.202060388

[96] F. Gao, C. Gao, S. He, Q. Wang, A. Wu, *Biosensors & bioelectronics* **2016**, *81*, 15-22.